IEEE Photonics Journal
An IEEE Photonics Society Publication

Open Access

Generation of Multiple Plasmon Resonances in a Nanochannel

Volume 5, Number 5, October 2013

Wei Peng
Yuzhang Liang
Lixia Li
Yun Liu
Jean-François Masson

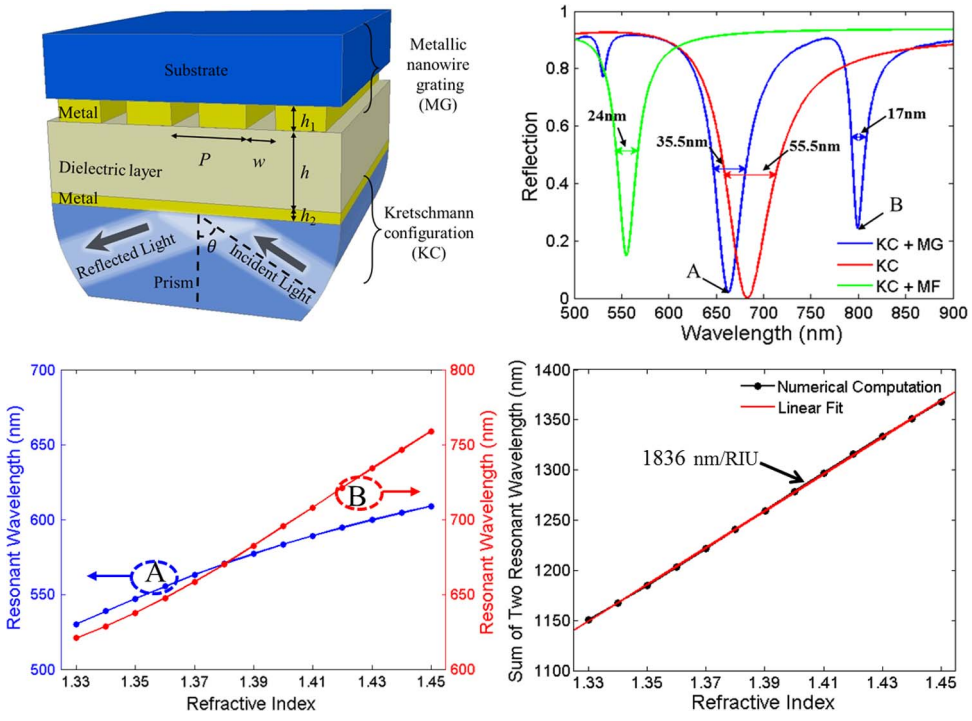

DOI: 10.1109/JPHOT.2013.2278983
1943-0655 © 2013 IEEE

IEEE photonics SOCIETY

IEEE

Generation of Multiple Plasmon Resonances in a Nanochannel

Wei Peng,[1] Yuzhang Liang,[1] Lixia Li,[1] Yun Liu,[1] and Jean-François Masson[2]

[1]College of Physics and Optoelectronics Engineering, Dalian University of Technology, Dalian 116024, China
[2]Department of Chemistry, University of Montréal, Montréal, QC H3C 3J7, Canada

DOI: 10.1109/JPHOT.2013.2278983

Manuscript received July 7, 2013; revised August 8, 2013; accepted August 14, 2013. Date of publication August 23, 2013; date of current version August 28, 2013. This work was supported by the National Nature Science Foundation of China under Grants 61137005 and 60977055, by the Ministry of Education of China (SRFDP), and by the National Science and Engineering Research Council of Canada (NSERC) through the Discovery Grant Program. Corresponding author: W. Peng (e-mail: wpeng@dlut.edu.cn).

Abstract: In this paper, we investigate the coupling of surface plasmon based on Kretschmann configuration (KC) to localized and delocalized surface plasmon modes supported by metallic nanowire grating (MG) at the oblique incidence. The designed structure consists of MG deposited on a substrate positioned upside down above a conventional KC at a certain distance. Mode coupling and resonant interactions between KC and MG create two new hybrid plasmon modes with narrow bandwidths and unique spectra features, resulting in two obvious dips in the reflection spectrum. Although both dips respond nonlinearly to the refractive index (RI) of the dielectric layer, surprisingly, the sum of two resonance wavelengths has a good linear approximation in a wider RI range. The simultaneous measurement of two resonance dips makes it more attractive as a surface plasmon resonance analysis technology, which is valuable for high-sensitivity optical sensors.

Index Terms: Nanostructures, plasmonics, subwavelength structures, theory and design, waveguides.

1. Introduction

Metallic nanostructures, with unique plasmonic properties, have received widespread attention in both fundamental and applied fields [1], [2]. Nanostructures have significant potential applications in many important areas such as nanoscale waveguides [3], filter, and plasmonic biosensors [4]. Recently, based on mutual coupling of plasmon–plasmon and light–plasmon, some intriguing optical phenomena have been demonstrated like negative permeability generated by paired metallic strips [5], plasmon–induced transparency [6]. The coupling between plasmon modes excited in complex metallic nanostructures provides a powerful approach to control and tailor the optical responses of the metallic nanostructures.

The coupling between metallic nanowire grating (MG) and metal film has been extensively studied [7]–[10]. When a thin metallic nanowire array (thickness smaller than penetration depth into metal) supporting localized surface plasmon (LSP) is placed close to a thin metal layer, the nanowire arrays allow the excitation of delocalized surface plasmon (DSP) on the metal layer surface. Because of the coupling between LSP and DSP, multiple resonance modes are observed in the extinction spectra [7]. When a dielectric Bragg reflector is added to above hybrid structure, Tamm plasmons are generated by the structure. The coupling of Tamm plasmons with LSP and DSP results in the new hybrid mode. DSP of metal film is excited through LSP supported by the MG. The coupling between these surface plasmons generates multiple resonance modes [8]. However, in

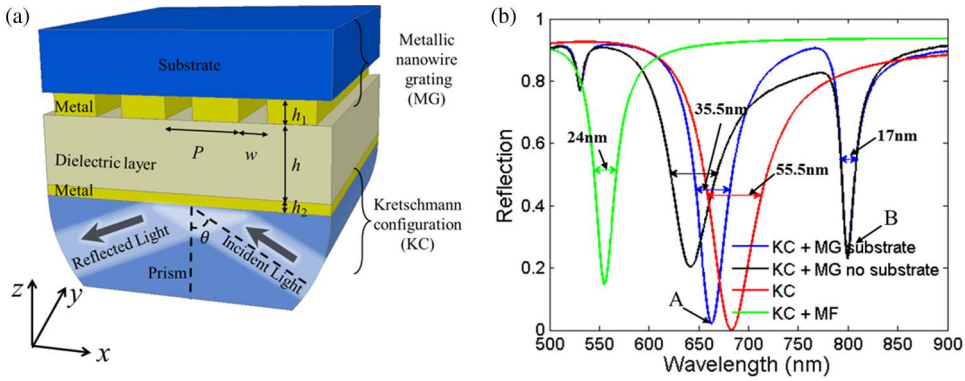

Fig. 1. Structure parameters of the KC/MG structure and its typical optical phenomenon. (a) Schematic diagram. (b) Reflection spectra (different structures).

the proposed nanostructure, a thick MG is introduced (thickness lager than penetration depth into metal). A thick MG can support the two surface plasmon modes: LSP and DSP modes. They are redefined as following in this paper: surface plasmon is excited on the top and down interface of metallic grating, which is named as DSP modes. The DSP excitation of metallic grating can lead to the emergence of minimum value in the transmission spectrum [11]; surface plasmon mode is confined inside the slit of grating, which is named as LSP mode. In this paper, the plasmon modes of MG are excited by the propagating surface plasmon of metal film, which distinguishes itself from other reported nanostructures [7]–[10].

Metallic nanostructures have been the focus of most concerns with small-volume, ultrasensitive sensors. Early studies mainly focused on the absolute shift of the plasmon peak by binding metallic nanostructures with the analytes [12]–[14]. However, the sensitivity enhancement in these structures is often accompanied with broadening of the plasmon peaks. To solve this bottleneck, some new plasmon structures are induced for the creation and utilization of narrow bandwidths for sensing application [15], [16], but these structures only provide single channel detection. Sherry *et al.* found two distinct plasmon resonance peaks by using a single silver nanocube on glass substrate [17]. Although two resonance peaks can be simultaneously applied for chemical detection, only peaks with shorter wavelength have good sensing capabilities. Moreover, compared to long wavelength peak, the peak with shorter wavelength with a relatively low peak depth is susceptible to structure parameters. We present a hybrid metallic nanostructure by combining a thin metal film with MG to generate two obvious resonance dips in one nanostructure. The two dips have narrow full width at half maximum (FWHM) and high depth. More interesting, the bulk refractive index (RI) sensitivity of our structure is comparable with that of Kretschmann configuration (KC), which is more sensitive than reported nanostructures [12]–[17]. The generation of multiple resonances in nanostructures will have great importance for realizing multichannel sensors.

In this paper, we propose a structure that can provide multiple resonance modes in which MG on a substrate is placed upside down on a dielectric layer deposited on a traditional KC (Fig. 1(a)). Our results show that there are two remarkable dips in the reflection spectrum, which is ascribed to the coupling of the surface plasmon from the KC with LSP and DSP modes supported by the MG. The influence of structure parameters on two resonance dips is also investigated. Moreover, both two resonance dips shift simultaneously as the RI of the dielectric layer changes. However, two resonance dips have different and complementary response characteristics to the RI of the dielectric layer, which result in a good linear approximation of the sum of two resonance wavelengths in a wider RI range.

2. Theoretical Model

Fig. 1 illustrates the operating principle of the proposed nanochannel based multiple resonances generation structure. Schematic diagram of the KC and MG hybrid nanostructure is depicted in

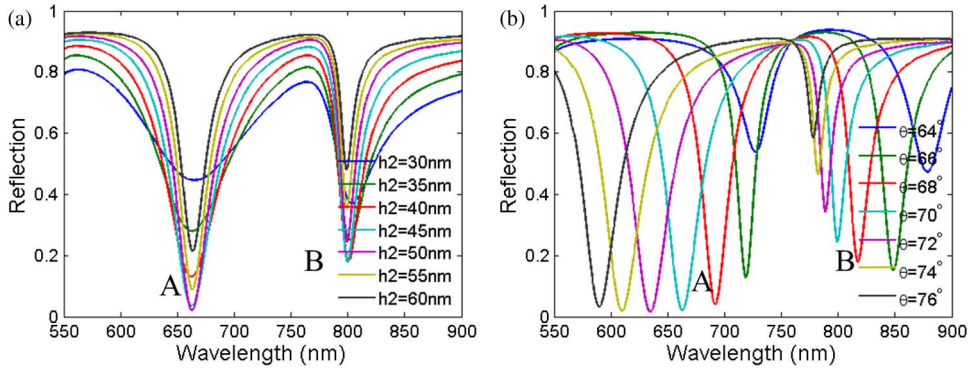

Fig. 2. Reflection spectra for (a) various metal film thickness h_2 and (b) different incidence angle θ. Other parameters are identical with that of blue line in Fig. 1(b).

Fig. 1(a). The parameters of the structure used here are: the thickness of metal film (MF) is $h_2 = 50$ nm; the period, slit width, and thickness of MG are $P = 320$ nm, $w = 120$ nm, and $h_1 = 200$ nm $(h_1 > 60$ nm$)$, respectively; a dielectric layer has a thickness of $h = 320$ nm and a RI of $n = 1.42$. The RI of the substrate and prism are 1.46 and 1.60, respectively. Silver used as metal material is described by a Drude–Lorentz model with related parameters according to Ref. [18].

We analyze the above design with a commercial FDTD solver [19]. To achieve high precision in the simulation, we use one period of the grating in the following calculation. For oblique incidence, the Bloch boundary conditions are used in x direction, and perfectly matched layer (PML) boundary conditions with 96 PMLs are used in z direction. Sub-gridding techniques are applied to obtain mesh cell resolutions down to 1×1 nm^2 in the metal region. The numerical calculations are performed with extremely well convergence condition. A plane wave with transverse magnetic polarization irradiates on the metal film from below the structure with a 70° incidence angle. Fig. 1(b) shows the reflection spectrum of the proposed KC/MG hybrid nanostructure (blue line). For comparison, the reflection spectrum for only KC is also shown (red line); and, using a metal film with the thickness 200 nm (MF) to replace the metallic grating (MG) in the KC/MG hybrid nanostructure, we constitute a KC/MF hybrid nanostructure. Its reflection spectrum is shown as a green line. There is only one dip in the reflection spectra of two reference structures calculated by using the matrix method for N-layer model. However, in the KC/MG structure, a new resonance dip (marked as B) appears at the longer wavelength region. Then, there are two obvious dips A and B in the reflection spectrum of our proposed structure. The FWHM of two dips are 35.5 and 17 nm, respectively, which are narrower than that of the only KC structure. Narrow resonance peak improves directly the RI resolution of SPR sensors and provides lower detection limits. Narrow resonance dips are important for sensitivity enhancement of surface plasmon sensing technology. Moreover, the reflection spectrum for the KC/MG hybrid nanostructure without substrate layer is shown in black line of Fig. 1(b). It can be seen that the position of dip B of black line is completely consistent with that of the blue line, but the position of dip A of two lines is a little different. It illustrates that both dips A and B still exist in the reflection spectrum when substrate layer of Fig. 1(a) is absent. Even substrate layer has no effect on the dip B, but it affects the depth and FWHM of dip A. It also illustrates that FWHM of dip A can be adjusted by changing the RI of substrate layer.

3. Results and Discussion

Fig. 2 presents reflection spectra of the designed structure with various metal film thickness and different incidence angle. As shown in Fig. 2(a), the FWHM of both resonance dips A and B can be tuned by selecting metal film thickness h_2. As h_2 increases, the FWHM of both dips decreases gradually, but when h_2 is larger than 45 nm, the depth of both dips decreases with the increase of h_2. Moreover, the metal film thickness h_2 has subtle influence on the position of dips A and B, which is consistent with the traditional SPR theory [20]. In Fig. 2(b), as incidence angle θ increases, both dips have a blue shift, which also agrees with the tradition SPR theory [1]. From Fig. 2(b), we find

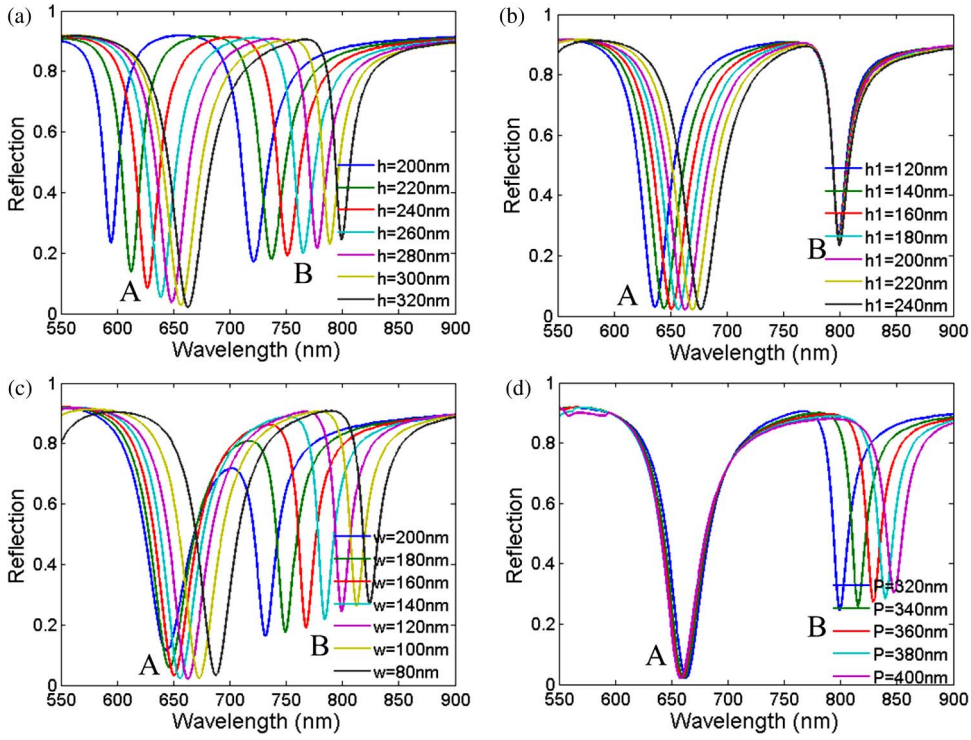

Fig. 3. Reflection spectra for different structure parameters with fixed $h_2 = 50$ nm and incidence angle 70°. (a) Varying the thickness of dielectric layer h with fixed $P = 320$ nm, $w = 120$ nm, and $h_1 = 200$ nm. (b) Varying the thickness of grating h_1 with fixed $P = 320$ nm, $w = 120$ nm, and $h = 320$ nm. (c) Varying the slit width of grating w with fixed $P = 320$ nm, $h_1 = 200$ nm, and $h = 320$ nm. (d) Varying the period of grating P with fixed $P - w = 200$ nm, $h_1 = 200$ nm, and $h = 320$ nm.

that an incidence angle within 68° to 72° is suitable for our structure. In order to simultaneously achieve narrower FWHM and higher dip depth of both dips A and B, we select the thickness of metal film h_2 as 50 nm and incidence angle θ as 70° in the following investigation.

The influence of different structure parameters on dips A and B is illustrated in Fig. 3. Fig. 3(a) shows that the wavelength position of both resonance dips can be tuned by varying the thickness of dielectric layer h. As h increases, both dips have red shifts. The depth of dip A increases gradually; on the contrary, the depth of dip B decreases gradually with the increase of h. When h becomes large, the coupling strength between the KC and MG is gently reduced, therefore the interaction between KC and MG decreases, which results in red shifts of both dips and the decrease of the depth for dip B. When h becomes large enough, the interaction between KC and MG becomes very small and eventually dip B disappears. It is clear that the emergence of dip B is caused by the interaction between evanescent waves excited on metal surface of KC and MG. Therefore, to enhance the interaction, we can increase the penetration depth of the evanescent wave in the dielectric layer by decreasing incidence angle of surface plasmon mode excited on metal surface of KC. As a result, the distance h of interaction between KC and MG can be increased greatly. In Fig. 3(b), the reflection spectra are plotted by changing the grating thickness h_1. As h_1 increases, only dip A shows a red shift and dip B keeps constant. It means that the grating height only influences the LSP mode generation in the slit of grating, and the change of LSP mode leads to the red shift of dip A. By contrast, Fig. 3(d) shows the effect from the MG period P. It is obvious that dip B makes red shift as P increases, but dip A has little dependence on the change of P. The influence of the slit width w on two resonance dips is exhibited in Fig. 3(c), the wavelength of both dips are red shifted simultaneously as w decreases. In Fig. 3(d), when keep the difference between P and w as a constant $P - w = 200$ nm, the increase of period will change slit width. Fig. 3(c) also shows that dip A has a red shift as w decreases. Then, it can be deduced that dip A is red shifted as period

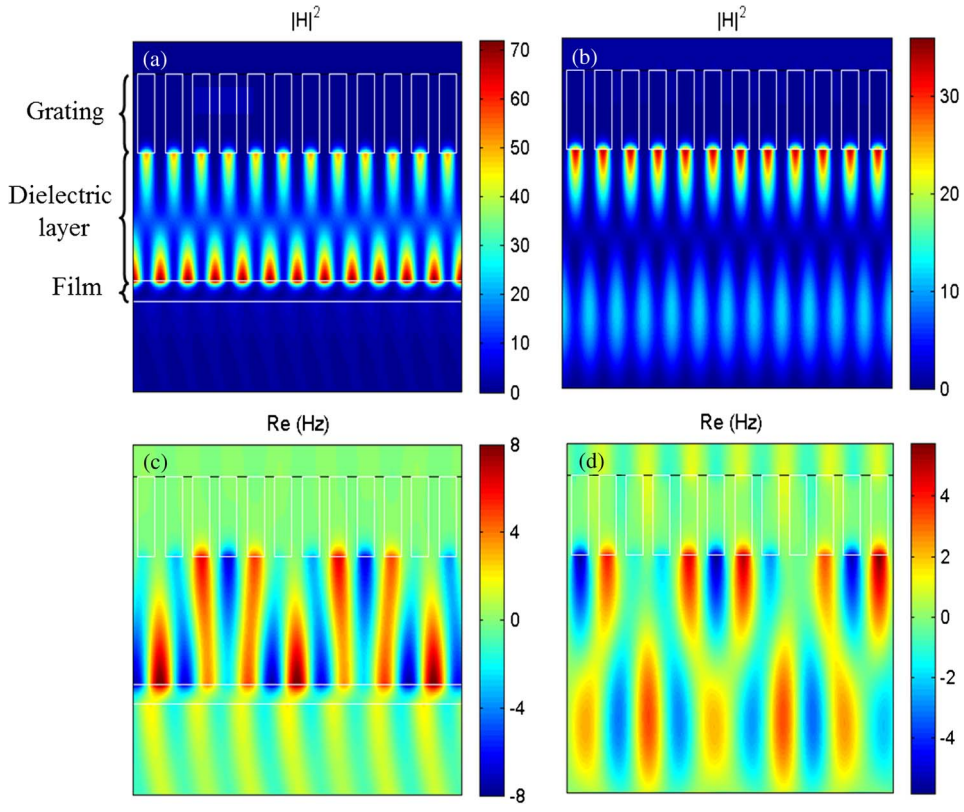

Fig. 4. Spatial field distribution of different structures. Magnetic intensity $(|H|^2)$ distribution of (a) KC/MG hybrid structure and (b) only metallic grating at the wavelength 800 nm. Real part of magnetic field (Re(Hz)) distribution of (c) KC/MG hybrid structure and (d) metallic grating.

of MG increases at a certain slit width w. Therefore, the periodicity (P) and slit width w of the nanochannel structure are key parameters to tuning the resonance position A, which is directly related with the LSP mode in the slit of nanochannel. Through these analyses, the position of dip A is mainly determined by the geometric parameters such as the thickness h_1, slit width w of MG, and period P; and the position of dip B is mainly determined by the period P and slit width w that related to properties of the MG top surface. We conclude that both dips A and B are originated from two coupling mechanisms independently, and there is no correlation between them. This multiple plasmon resonance character is distinguished from previous works [7]–[10], which is valuable for multichannel SPR sensing, and more explanation is presented in the following part.

To further understand the underlying physics of two resonance dips, the magnetic intensity $(|H|^2)$ and the real part of magnetic field (Re(Hz)) at the wavelength of dip B are investigated as shown in Fig. 4(a) and (c), respectively. Fig. 4(a) and (c) indicate that the magnetic field is almost confined and propagates inside the dielectric layer, which reaches its maximum on the surface of metal film and metallic grating at the wavelength of dip B. Furthermore, we observe the exponential dependence of field in the vertical direction and the periodic distribution of field in horizontal direction on both surfaces. These unique properties are very similar to that of DSP mode supported by MG. From Fig. 4(b) and (d), the magnetic intensity $(|H|^2)$ and the real part of magnetic field corresponding to the excited surface plasmon mode at the wavelength 800 nm on the surface of MG alone (no KC). The parameters of MG are identical to that of Fig. 1(a) except for a different incidence angle of 46.2°. These parameters are satisfied with surface plasmon excitation condition of the MG [11], [21]

$$\frac{2\pi}{\lambda} n_{sl} \sin\theta_1 - m\frac{2\pi}{P} = -\frac{2\pi}{\lambda}\sqrt{\frac{\varepsilon_m(\omega) n_{sl}^2}{\varepsilon_m(\omega) + n_{sl}^2}} = k_{spp} \tag{1}$$

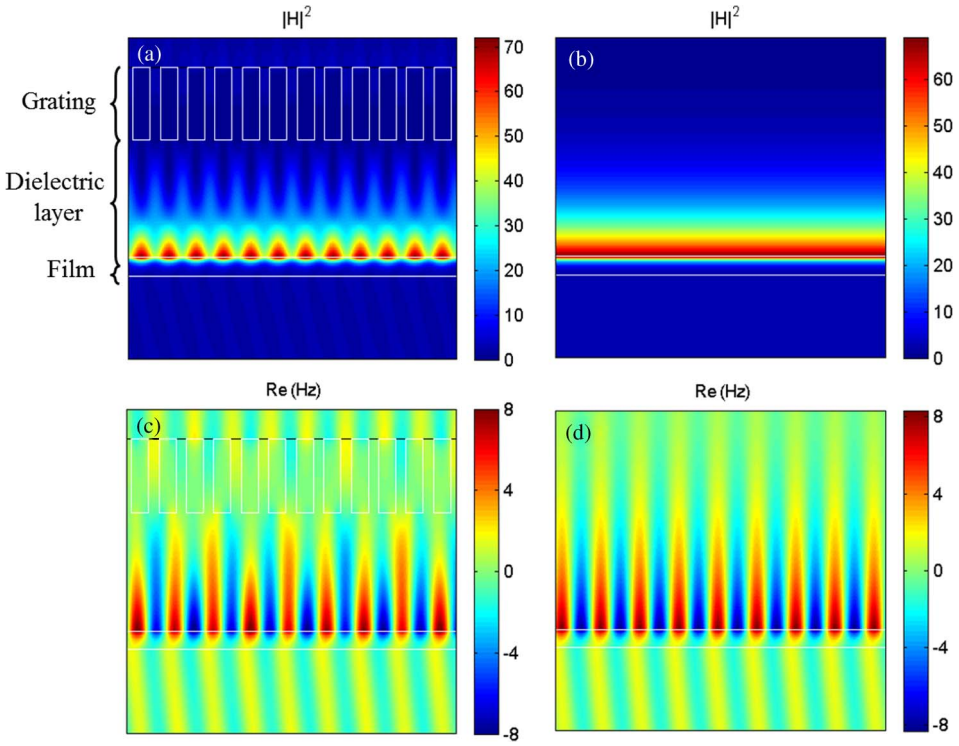

Fig. 5. Magnetic intensity ($|H|^2$) distribution of (a) KC/MG hybrid structure at the wavelength 663 nm and (b) only KC at the wavelength 683 nm. Real part of magnetic field (Re(Hz)) distribution of (c) KCMG hybrid structure at the wavelength 663 nm and (d) KC at the wavelength 683 nm.

where $m = 1$ is the diffraction order; $n_{sl} = 1.42$ is RI of dielectric layer; $P = 320$ nm is metallic grating period; $n_{sub} = 1.46$ is RI of substrate; and ε_m is permittivity of metal silver [18]. At above resonance condition, the energy carried by the incident wave can be transferred to the SPPs, which propagates along the grating/dielectric interface. Field distribution in the grating surface of Fig. 4(b) and (d) is nearly identical to that shown in Fig. 4(a) and (c). It illustrates that DSP is satisfied in this MG, and surface plasmon wave propagates along the metallic grating/dielectric interface. But in Fig. 4(a) and (c), surface plasmon wave on grating/dielectric interface is influenced by the thin metal film, and it also propagates along thin metal film/dielectric interface simultaneously, which is similar to that on the grating/dielectric interface. As a result, the dip B in the reflection spectrum also can be affected by the metal film. Therefore, we conclude that the dip B in the reflection spectrum is induced by the coupling between DSP mode of the MG and the excited evanescent wave of the KC.

We analyze and compare the magnetic field distributions of KC/MG structure with KC only structure in Fig. 5. The corresponding magnetic intensity ($|H|^2$) and the real part of magnetic field (Re(Hz)) for the wavelength 663 nm of dip A are displayed in Fig. 5(a) and (c). As a comparison, Fig. 5(b) and (d) demonstrates the field distribution of SPR of the KC at the wavelength of 683 nm; the dip of the red line in Fig. 1(b) is satisfied with surface plasmon resonance condition [1]:

$$\frac{2\pi}{\lambda} n_{prism} \sin\theta = \mathrm{Re}\left[\frac{2\pi}{\lambda}\sqrt{\frac{\varepsilon_m(\omega) n_{sl}^2}{\varepsilon_m(\omega) + n_{sl}^2}}\right] \tag{2}$$

Fig. 5(a)–(d) demonstrates that the field distribution of dip A of the proposed structure is similar to that of traditional SPR, but the periodicity of the field intensity (Fig. 5(a)) of dip A in horizontal direction is affected by the tailored role of MG. The emergence of dip A is mainly associated to the SPR at the surface of metal and dielectric, however, the SPR is influenced by the MG. Combining Fig. 3 with Fig. 5(a)–(d), the position of dip A can be tuned by the thickness h_1 and slit width w, and

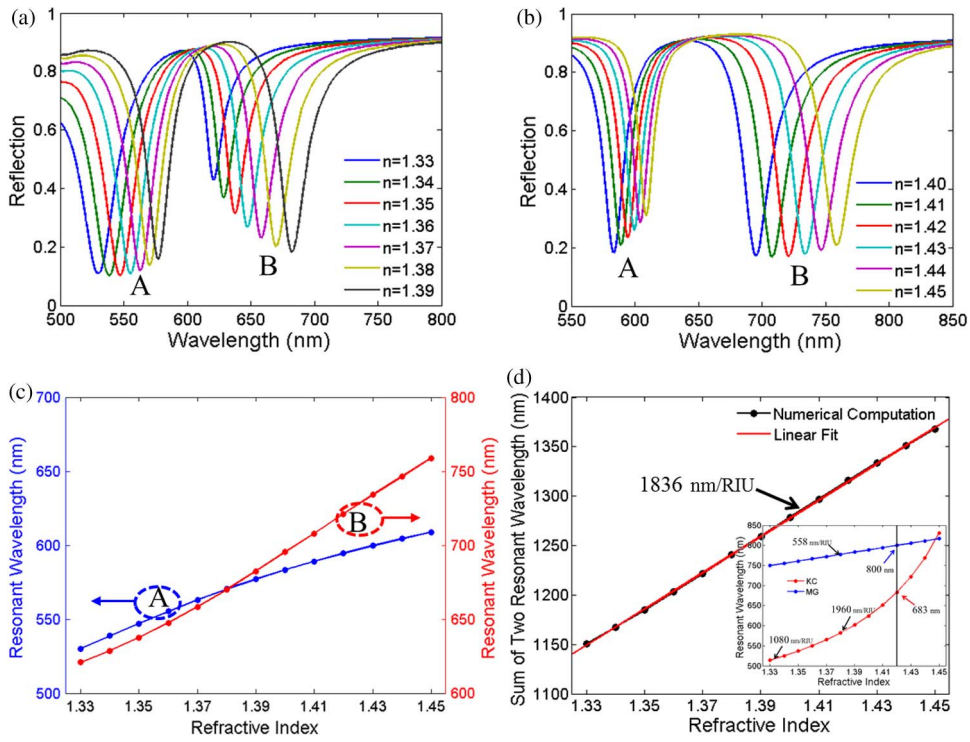

Fig. 6. (a) and (b) Reflection spectra of the proposed structure with various refractive index (RI) of dielectric layer. (c) Wavelength response of two different resonance dips with various RI. (d) RI response of the sum of two resonance wavelengths. Inset depicts RI response of traditional KC and MG structures.

it can be concluded that dip A is affected by LSP modes inside the slits of grating. Therefore, the physics of dip A should be mainly ascribed to the coupling of SPR of the KC and the LSP modes inside the slits of MG (Fig. 3(b)). Additionally, most of energy at the two dips is confined in the dielectric layer, and there are two remarkable peaks in the absorption spectrum, which can be used in design of optical absorber.

As shown in Fig. 6, two resonance dips can be tuned by changing the RI of the dielectric layer of the proposed structure. The structure parameters are identical to that of Fig. 1(a) except for the dielectric layer thickness h is 200 nm. Reflection spectra of the structure with a wide RI ranging from 1.33 to 1.45 are shown in Fig. 6(a) and (b), which illustrates that both dips maintain narrow FWHM and high depth in the wide RI range. Narrow FWHM and high depth are two crucial factors for high sensitivity sensing application. Fig. 6(c) presents wavelength positions of two resonance dips A (blue dots line) and B (red dots line) as the reflective index n of the dielectric layer, which also demonstrates that wavelength shifts of dips A and B are nonlinear with the change of reflective index n of the dielectric layer. More specifically, the rate of wavelength shift becomes smaller for dip A, but gets larger for dip B; also as shown in Fig. 6(d), the numerical sum of two resonance wavelengths has a good linear approximation in the RI range from 1.33 to 1.45. It indicates that simultaneous measurement of these two resonance dips can greatly improve the linearity and sensitivity (nm/RIU) of the sensor measurement. Usually, it is difficult that SPR sensors based on single thin metal layer or bimetallic layer own both good linearity and high sensitivity in the larger RI range [22]. Two resonance dips A and B have complementary response to the RI of the dielectric layer, which is applied to tackle the difficult problem.

It is well known that usually two fundamental mechanisms are used to generate surface plasmon polaritons: prism coupling from KC structure and grating coupling from MG. As shown in the inset of Fig. 6(d), based on Eqs. (1) and (2), RI response of traditional KC and MG structures is represented by red solid line and blue solid line, respectively. The corresponding sensitivity of two structures is

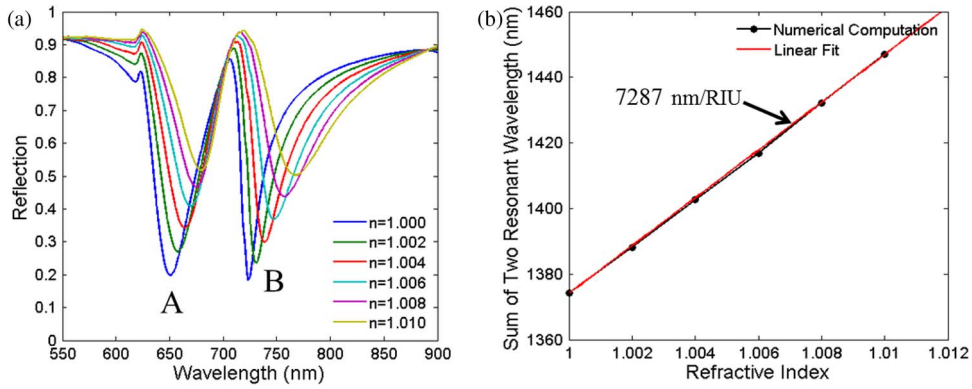

Fig. 7. (a) Reflection spectra of the proposed structure with various refractive index (RI) of dielectric layer. (b) RI response of the sum of two resonance wavelengths. Dielectric layer is replaced by air layer.

also shown in the inset of Fig. 6(d). The KC based SPR structures have high sensitivities but are nonlinear to RI changes (Fig. 6(d)), while the MG based sensor has lower sensitivity (558 nm/RIU) but good linearity to RI response. The hybrid structure based SPR design we presented as above can provide both high sensitivity (1836 nm/RIU) and good linearity by integrating these two traditional SPP coupling methods and overcoming their drawbacks or limitations.

We expect that this nanochannel based structure can be applied in dual or multiple channel gas sensor development. As shown in Fig. 7, the optical response remains similar with air as the dielectric layer and the corresponding adjustment of metallic grating parameters. Two obvious dips A and B still appear in the reflection spectrum of our designed structure. As shown in Fig. 7(b), the numerical sum of two resonance wavelengths has a good linear approximation and high sensitivity in the larger RI range from 1 to 1.01 (Fig. 7(b)). It further proves that the above results are correct. All above results are achieved when substrate layer is placed on the MG. Moreover, in agreement with the physics of the device, the emergence of two dips is not directly related to the nature of the substrate layer. As mentioned in Fig. 1(b), it may be applied in many aspects. Hydrogen sensing is a good example. For this sensor, the dielectric layer can be replaced by any sensitive material to hydrogen presenting an optical change. Sensitive material such as Pd alloys, Pd nanoparticles oxide materials (WO_3, Pd_2VO_5), or Mg alloys with a cap layer of Pd could be envisioned. For example, Nau *et al.* reported that hydrogen sensor is implemented with the change of optical properties of waveguide layer by gasochromic mechanisms [23] and tungsten trioxide (WO_3) is used as a waveguide layer below a thin metal grating. Our designed structure is also expected to work as a sensitive hydrogen sensor by substituting dielectric layer for tungsten trioxide. Although structures are similar, the operating principle of structures is entirely different.

4. Conclusion

In summary, we demonstrated a novel sensor structure which can provide multiple resonances based on a combination of KC and MG. Different mode coupling and resonance interactions generate two notable resonance dips. Both dips have narrow FWHM and high depth and have good linear RI response. Further optimization of this structure can achieve more resonances. The proposed design can be further developed as a high-sensitivity multichannel nanostructure sensing method, which can find applications in RI measurement especially for chemical gas detection.

References

[1] S. A. Maier, *Plasmonics: Fundamentals and Applications*. New York, NY, USA: Springer, 2007.
[2] W. L. Barnes, A. Dereux, and T. W. Ebbesen, "Surface plasmon subwavelength optics," *Nature*, vol. 424, pp. 824–820, Aug. 2003.
[3] P. Neutens, P. V. Dorpe, I. D. Vlaminck, L. Lagae, and G. Borghs, "Electrical detection of confined gap plasmons in metal–insulator–metal waveguides," *Nature Photon.*, vol. 3, pp. 283–286, 2009.

[4] N. Liu, T. Weiss, M. Mesch, L. Langguth, U. Eigenthaler, M. Hirscher, C. Sonnichsen, and H. Giessen, "Planar metamaterial analogue of electromagnetically induced transparency for plasmonic sensing," *Nano Lett.*, vol. 10, no. 4, pp. 1103–1107, 2010.
[5] V. M. Shalaev, W. Cai, U. K. Chettiar, H.-K. Yuan, A. K. Sarychev, V. P. Drachev, and A. V. Kildishev, "Negative index of refraction in optical metamaterials," *Opt. Lett.*, vol. 30, no. 24, pp. 3356–3358, 2005.
[6] N. Liu, L. Langguth, T. Weiss, J. Kastel, M. Fleischhauer, T. Pfau, and H. Giessen, "Plasmonic analogue of electromagnetically induced transparency at the Drude damping limit," *Nature Mater.*, vol. 8, pp. 758–762, 2009.
[7] R. Ameling, D. Dregely, and H. Giessen, "Strong coupling of localized and surface plasmons to microcavity modes," *Opt. Lett.*, vol. 36, no. 12, pp. 2218–2220, 2011.
[8] H. Liu, X. Sun, F. Yao, H. Yuan, and H. Zhao, "Controllable coupling of localized and propagating surface plasmons to Tamm plasmons," *Plasmonics*, vol. 7, pp. 749–754, 2012.
[9] A. Christ, T. Zentgraf, S. G. Tilhodeev, N. A. Gippius, J. Kuhl, and H. Giessen, "Controlling the interaction between localized and delocalized surface plasmon modes: Experiment and numerical calculations," *Phys. Rev. B*, vol. 74, no. 15, pp. 155435-1–155435-8, 2006.
[10] J. Chen, P. Wang, Z. Zhang, Y. Lu, and H. Ming, "Coupling between gap plasmon polariton and magnetic polariton in a metallic–dielectric multilayer structure," *Phys. Rev. E*, vol. 84, no. 2, pp. 026603-1–026603-9, Aug. 2011.
[11] Y. Liang, W. Peng, R. Hu, and H. Zou, "Extraordinary optical transmission based on subwavelength metallic grating with ellipse walls," *Opt. Exp.*, vol. 21, no. 5, pp. 6139–6152, Mar. 2013.
[12] W. C. Law, K. T. Yong, A. Baev, and P. N. Prasad, "Sensitivity improved surface plasmon resonance biosensor for cancer biomarker detection based on plasmonic enhancement," *ACS Nano*, vol. 5, no. 6, pp. 4858–4864, 2011.
[13] W. C. Law, K. T. Yong, A. Baev, R. Hu, and P. N. Prasad, "Nanoparticle enhanced surface plasmon resonance biosensing: Application of gold nanorods," *Opt. Exp.*, vol. 17, no. 21, pp. 19041–19046, 2009.
[14] D. E. Mustafa, T. Yang, Z. Xuan, S. Chen, H. Tu, and A. Zhang, "Surface plasmon coupling effect of gold nanoparticles with different shape and size on conventional surface plasmon resonance signal," *Plasmonics*, vol. 5, no. 3, pp. 221–231, Sep. 2010.
[15] E. M. Hicks, S. Zou, G. C. Schatz, K. G. Spears, and R. P. Van Duyne, "Controlling plasmon line shapes through diffractive coupling in linear arrays of cylindrical nanoparticles fabricated by electron beam lithography," *Nano Lett.*, vol. 5, no. 6, pp. 1065–1070, 2005.
[16] S. Zou and G. C. Schatz, "Narrow plasmonic/photonic extinction and scattering line shapes for one and two dimensional silver nanoparticle arrays," *J. Chem. Phys.*, vol. 121, no. 24, pp. 12606–12612, Dec. 2004.
[17] L. J. Sherry, S. H. Chang, G. C. Schatz, R. P. Van Duyne, B. J. Wiley, and Y. Xia, "Localized surface plasmon resonance spectroscopy of single silver," *Nano Lett.*, vol. 5, no. 10, pp. 2034–2038, 2005.
[18] S. G. Rodrigo, F. J. García-Vidal, and L. Martín-Moreno, "Influence of material properties on extraordinary optical transmission through hole arrays," *Phys. Rev. B*, vol. 77, no. 7, pp. 075401-1–075401-8, 2008.
[19] *Lumerical Solutions*. [Online]. Available: http://www.lumerical.com
[20] H. Raether, *Surface Plasmons on Smooth and Rough Surfaces and on Gratings*. Berlin, Germany: Springer, 1988.
[21] Y. Liang and W. Peng, "Theoretical study of transmission characteristics of sub-wavelength nano-structured metallic grating," *Appl. Spectrosc.*, vol. 67, no. 1, pp. 49–53, 2013.
[22] A. K. Sharma and B. D. Gupta, "On the performance of different bimetallic combinations in surface plasmon resonance based fiber optic sensors," *J. Appl. Phys.*, vol. 101, no. 9, pp. 093111-1–093111-6, 2007.
[23] D. Nau, A. Seidel, R. B. Orzekowsky, S. H. Lee, S. Deb, and H. Giessen, "Hydrogen sensor based on metallic photonic crystal slabs," *Opt. Lett.*, vol. 35, no. 18, pp. 3150–3152, 2010.